CROATICA CHEMICA ACTA
CCACAA, ISSN 0011-1643, e-ISSN 1334-417X
Croat. Chem. Acta **85** (4) (2012) 435–439.
http://dx.doi.org/10.5562/cca2108

Original Scientific Article

High Resolution Structure of the Manganese Derivative of Insulin†

Biserka Prugovečki,* Ivana Pulić, Martina Toth, and Dubravka Matković-Čalogović

Division of General and Inorganic Chemistry, Department of Chemistry, Faculty of Science, University of Zagreb, Horvatovac 102a, HR-10000 Zagreb, Croatia

RECEIVED JUNE 19, 2012; REVISED OCTOBER 2, 2012; ACCEPTED OCTOBER 3, 2012

Abstract. The structure of the human manganese derivative of insulin was determined using the single crystal X-ray diffraction method. Single crystals were grown by the hanging drop vapour diffusion crystallization method using zinc-free insulin and manganese(II) sulphate monohydrate in citrate buffer at pH = 6.4. It crystallizes in the trigonal system in the space group *R* 3 with the unit cell parameters: $a = b =$ 81.70 Å and $c = 33.73$ Å. There are two manganese ions per insulin hexamer in the human manganese-insulin derivative. The manganese ions lie on the three-fold crystallographic axis on opposite sides of the hexamer. Both manganese ions are octahedrally coordinated by three $N^{\varepsilon 2}$ atoms from the imidazolyl side chains of three symmetry-related HisB10/HisD10 and three oxygen atoms of three symmetry-related water molecules. The investigated human manganese-insulin derivative adopts the T_6 conformation. (doi: 10.5562/cca2108)

Keywords: insulin derivative, manganese, X-ray structure

INTRODUCTION

Insulin is a peptide hormone that regulates the level of glucose in the blood and is a therapeutic protein that is used medically for the treatment of diabetes mellitus. Insulin is structured of two polypeptide chains with chain A consisting of 21 and chain B of 30 amino acids. Chains A and B are linked by two disulphide bonds, while the third intrachain disulphide bond links residues A6 and A11. Metal ions have important implications on insulin storage, release and conformation. Insulin storage vesicles in many species contain high concentrations of Zn^{2+} and Ca^{2+} ions and insulin is accumulated in the pancreas as a Zn^{2+} containing hexamer. Hexamer formation is related to insulin storage and to some of processes in its biosynthesis.[1–3] There are three forms of insulin hexamers named T_6, $T_3R_3^f$ and R_6. These notations refer to the folding of the N-terminal part of the B chains in insulin hexamers.[4] The T_6 conformation is obtained at low chloride concentrations and in absence of phenolic derivatives.[5–7] The T_6 insulin hexamer has two high-affinity metal ion binding sites which are located on the 3-fold axis and each metal ion is octahedrally coordinated by three His B10 residues (one from each dimer) and three water molecules. It has been shown that chloride ions induce the T to R transition at residues B4-B8 in three molecules out of six in the insulin hexamer forming the $T_3R_3^f$ hexamer.[8,9] It was found that $T_3R_3^f$ type of hexamer can contain a different number of Zn^{2+} ions per hexamer with different coordination. When phenol or phenolic derivatives are included in the crystallization solution, all six B chain N termini adopt a α-helical conformation, termed the R_6 hexamer form.[10–13] Many structural studies on chemically and genetically modified insulins have been done. It has been known for many years that different metal ions can substitute zinc ions in the T_6 hexamer.[14] The zinc binding cavities in the insulin hexamer can accommodate different metal ions which prefer imidazole and water molecule ligands.[15–19] As a part of our ongoing research on the crystallization and structural studies on human insulin derivatives[17,18] in the present study the zinc ions in human insulin were substituted with manganese.

Manganese is a trace mineral that takes part in wide range of metabolic function. The human body contains approximately ten miligrams of manganese, and it is a cofactor for a number of enzymes like arginase, pyruvate carboxylase, mitochondrial superoxide dismutase and several peptidases and glycosyltransferases.[20–22] Prothrombin and vitamin K are formed with the help of manganese and it is also important for the body's utilization of vitamin E.

The crystal structure of Mn^{2+} arg-insulin hexamer (a modified form of insulin in which an arginine residue

† This article belongs to the Special Issue devoted to the 85th anniversary of *Croatica Chemica Acta*.

* Author to whom correspondence should be addressed. (E-mail: biserka@chem.pmf.hr)

is attached to the N-terminal of the A-chain of human insulin) was recently reported as a $T_3R_3^f$ hexamer.[15] We report here the crystal structure of hexameric T_6 human manganese-insulin derivative.

EXPERIMENTAL

Crystallization

Crystals of the human manganese-insulin derivative were grown by the hanging drop vapour diffusion method. Chemicals employed in the crystallization study were reagent grade or better and were used without further purification. Zinc-free biosynthetic human insulin was used. Optimum crystallization conditions are as follows: the protein solution consisted of 7.5 mg mL^{-1} of zinc-free insulin in 0.02 mol L^{-1} HCl; the reservoir solution was at pH = 6.4 containing sodium citrate (1 mmol L^{-1}), acetone ($\varphi = 10$ %), $MnSO_4 \cdot H_2O$ (9 mmol L^{-1}) and redistilled water. Each drop consisted of 1μL of protein solution and 1μL of reservoir solution. Colourless, sharp-edged rhombohedrons up to 0.4 mm in length grew in 4 days at $T = 291$ K.

Diffraction Data Collection

Intensity data for the human manganese-insulin derivative were collected on a single crystal cryoprotected by immersing it in the solution consisting of a volume fraction of $\varphi = 70$ % reservoir solution and $\varphi = 30$ % ethylene-glycol. The low temperature diffraction data to 1.08 Å resolution were collected with oscillation angles of 1.0 ° at the ELETTRA Synchrotron Light Laboratory, beam-line XRD-1 (wavelength, λ = 1.00 Å) using a CCD detector from MAR Research and an Oxford Cryosystems cryocooler. The data were processed with MOSFLM[23] and then scaled and merged by use of the CCP4 suite.[24] Data statistics are given in Table 1.

X-ray Analysis and Structure Refinement

The T_6 human nickel insulin derivative[17] from which all water molecules, nickel ions and alternate side chains were omitted was taken as a starting model for refinement. Initially only 4 Å resolution data were included in the rigid body refinement. The largest peaks from the initial F_o - F_c map corresponded to a pair of manganese atoms located on the three-fold axis. The structure was then refined at a higher resolution using maximum-likelihood minimization implemented in REFMAC[25] with 5 % of the total data being excluded for the purpose of the R_{free} refinement. Program COOT[26] was used to fit the model into the electron density map ($2F_o$ - F_c and F_o - F_c maps). Water molecules were added by the ARP/wARP program[27] and were checked in accord with the criteria of electron density and acceptable hydrogen bonds to other atoms. The final refinement was carried out using anisotropic displacement parameters. Side chains SerA9, ValB12, ThrB27, SerD9, ValD12 were refined in two alternative conformations with occupancies of 50 %. Low density was observed for the terminal atoms of the side chain of PheD1, ValD2 and LysD29. The refinement converged at R = 0.159 and R_{free} = 0.194. The final model consists of 844 protein atoms, 189 water molecules, two manganese, and one sodium ion. The model has good stereochemistry, the r.m.s. deviations for bond lengths and bond angles are 0.027 Å and 2.4 °, respectively. In the Ramachandran plot 97.53 % of the residues are in the preferred regions and 2.47 % in allowed regions. The crystallographic data and structure

Table 1. Data measurement and refinement statistics for the T_6 human manganese-insulin derivative

Space group	$R\,3$
Unit cell parameters	
$a = b$ / Å	81.70
c / Å	33.73
$\alpha = \beta$ / °	90
γ / °	120
Temperature / K	100
$\langle B_{iso} \rangle$ / Å^2	8.583
No. of frames	120
Resolution / Å	10.3–1.08
Completeness / %	96.7
No. of unique reflections	43875
No. of free reflections	1770
Overall R_{merge}	0.089
Mean (I / σI)	11.0
Refinement statistic	
R	0.159
R_{free}	0.194
Cross-validated σ_A estimated error / Å	0.129
R.m.s. deviations from ideal	
Bond lengths / Å	0.027
Bond angles / °	2.4
Dihedral angles / °	7.0
Highest resolution shell	
Resolution range / Å	1.108–1.080
No. of reflections	5824
Completeness / %	87.3
R	0.233
R_{free}	0.299
Mean (I / σI)	6.3

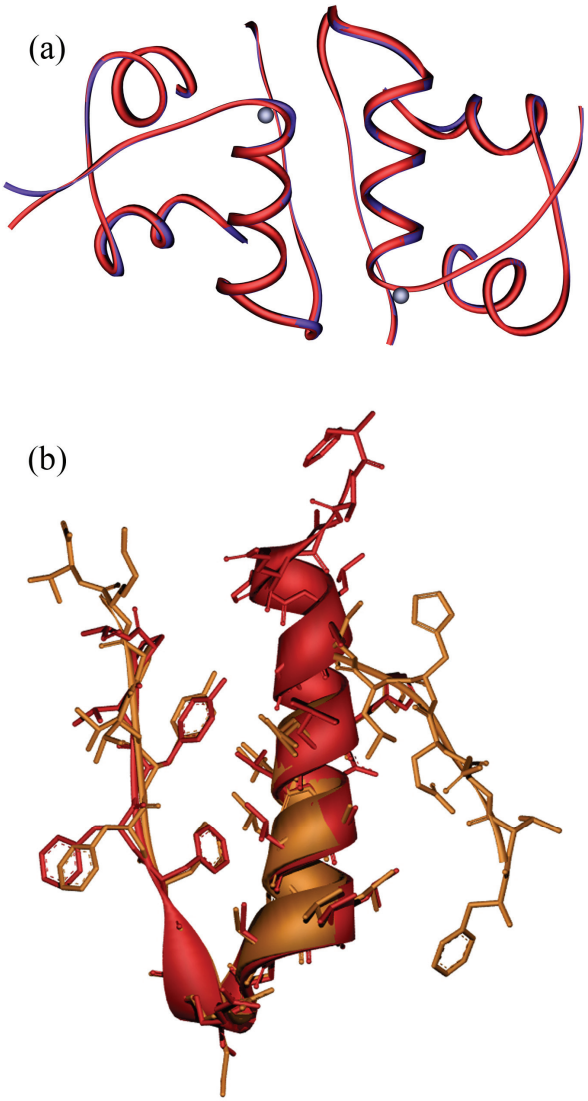

Figure 1. Cartoon representation of the superposed T_2 Mn^{2+}-insulin derivative (red) and T_2 Zn^{2+} insulin derivative (blue). Manganese and zinc ions are shown as spheres (a). The cartoon representation of the superposed B chain of the $T_3R_3^f$ Mn^{2+} arg-insulin (red) with the same chain in the the T_6 Mn^{2+} insulin (orange) (b).

refinement statistics are given in Table 1. The geometry of the model was monitored with PROCHECK.[28] The structure drawings were done by the PyMOL[29] program and Discovery Studio 3.1 Visualizer.[30]

RESULTS AND DISCUSSION

Dimer and Hexamer Conformation

Unlike the crystal structure of the Mn^{2+} arg-insulin[15] hexamer which was reported as $T_3R_3^f$, the investigated human manganese-insulin derivative adopts a T_6 conformation like in the native Zn^{2+} insulin derivative.[6] The superposition of the T_2 Mn^{2+} insulin derivative and T_2 native Zn^{2+} insulin derivative is shown in Figure 1a, while the superposition of the B chain of the $T_3R_3^f$ Mn^{2+} arg-insulin with the B chain of T_6 Mn^{2+} insulin derivative is shown in Figure 1b.

In the crystal structure the asymmetric unit consists of one T_2 dimer resulting in three T_6 insulin hexamers in the unit cell. The dimer is asymmetrical because the B25Phe side chain turns away from the two fold axis and contacts D25Phe across the two-fold axis. The same asymmetry at B25 is present in the native T_6 Zn^{2+} insulin[6]. The root mean square displacement between the T_2 dimer of investigated human manganese-insulin derivative and the TR^f Mn^{2+} arg-insulin derivative calculated using the CCP4 program LSQKAB[31] is given in Table 2, indicating the major structural difference in the B chain of the dimer molecules. Chains A, B, and C in the native T_2 zinc dimer[6] and the T_2 dimer of investigated human manganese-insulin derivative are similar within the limits of experimental error. The greatest main chain difference between those structures was found in the D chain (Table 2).

Coordination of Manganese Ions

It is well known that the T_6 insulin hexamer with Zn ions has two high-affinity metal ion binding sites which are located on the 3-fold axis and each metal ion is octahedrally coordinated by three $N^{\varepsilon 2}$ atoms from the

Table 2. Root mean square differences (expressed in Å) between the T_2 dimer of the investigated human manganese-insulin derivative, the TR^f Mn^{2+} arg-insulin derivative and the T_2 zinc insulin

	TR^f Mn^{2+} arg-insulin			T_2 zinc insulin		
Residue range	All atoms	C^α atoms	Main chain	All atoms	C^α atoms	Main chain
A chain	1.65	1.14	1.19	0.76	0.07	0.24
B chain	6.67	5.84	5.68	0.86	0.10	0.12
C chain	1.29	0.42	0.46	0.46	0.10	0.20
D chain	3.20	2.70	2.50	1.40	1.13	1.19

Table 3. Bond lengths (expressed in Å) between the octahedrally coordinated metal ions (Mn^{2+} or Zn^{2+}) and $N^{\varepsilon 2}$ atoms from the imidazolyl side chains of three HisB10 / HisD10 and oxygen atoms of water molecules in T_2 dimer of the investigated human manganese-insulin derivative and the T_2 zinc insulin

	T_2 Mn^{2+} insulin		T_2 Zn^{2+} insulin	
Mn–$N^{\varepsilon 2}$	2.09	2.14		
Mn–O	2.19	2.21		
Zn–$N^{\varepsilon 2}$			2.09	2.10
Zn–O			2.20	2.23

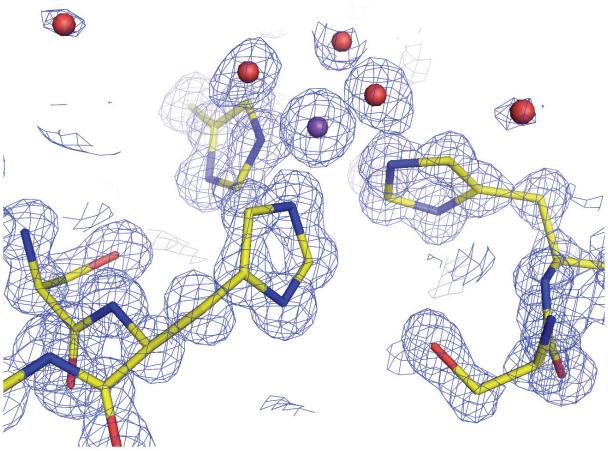

Figure 2. Coordination around the manganese ion showing the electron density: manganese atom (violet) is octahedrally coordinated by three $N^{\varepsilon 2}$ atoms from the imidazolyl side chains of three symmetry-related HisB10 and three oxygen atoms of three symmetry-related water molecules (red). The $2F_o$-F_c map is contoured at 1.4 σ.

imidazolyl side chains of three symmetry-related HisB10/HisD10 and three oxygen atoms of three symmetry-related water molecules.[5–7,16–18] The same coordination is found in the present Mn^{2+} insulin structure (Figure 2). So far, only in T_6 $4Ni^{2+}$ human arg-insulin crystal structure a dual octahedral and tetrahedral coordination of nickel ion is found at one site.[15] In the Mn^{2+} arg-insulin structure a tetrahedral coordination of Mn ion is observed (three $N^{\varepsilon 2}$ atoms from the imidazolyl side chains of three symmetry-related HisB10/HisD10 and a chloride ion).[15] Bond lengths between the octahedrally coordinated metal ions (Mn^{2+} or Zn^{2+}) and $N^{\varepsilon 2}$ atoms from the imidazolyl side chains of three HisB10 / HisD10 and oxygen atoms of water molecules in T_2 dimer of the investigated human manganese-insulin derivative and the T_2 zinc insulin are very similar (Table 3). The B10 to D10 manganese distance found in the T_6 manganese derivative is 16.44 Å while in the Mn^{2+} arg-insulin structure it was found to be 15.92 Å and in the native T_6 human insulin the distance between two zinc ions is 16.42 Å.

An analysis of the Protein Data Bank[32] with the crystal structures containing an octahedrally coordinated manganese ion with histidine as a ligand was carried out using the MESPEUS,[33] a database of the geometry of metal sites in proteins. Only structures with resolution ≤ 2.0 Å were investigated. There were 463 hits having octahedrally coordinated manganese ion with histidine as a ligand of which 29 structures had three histidines as ligands. In 9 structures three histidines and one or two water molecules were found as ligands to manganese.

The Cambridge Structural DataBase[34] search using the ConQeust Version 1.14, gave 15 structures of small molecules containing octahedrally coordinated manganese ion with three water molecules and three N-donor atoms. The Mn–N bond lengths are in the range of 2.117–2.431 Å and the Mn-O bond lengths in those structures are in the range of 2.128–2.349 Å.

CONCLUSION

The results show that the investigated manganese-insulin derivative adopts the T_6 conformation with two manganese ions located on the 3-fold axis separated by a distance of 16.44 Å. Both manganese ions are octahedrally coordinated by three $N^{\varepsilon 2}$ atoms from the imidazolyl side chains of three symmetry-related HisB10/HisD10 and three oxygen atoms of three symmetry-related water molecules. T_6 form of manganese-insulin derivative was compared with the $T_3R_3^f$ form of the Mn^{2+} arg-insulin structure and difference in hexamer conformation as well as metal coordination was found.

Supplementary Materials. – The coordinates and structure factor data for the reported manganese-insulin derivative have been submitted to the Protein Data Bank; PDB code 4FKA.

Acknowledgements. Financial support for this research was provided by the Ministry of Science, Education and Sports of the Republic of Croatia (Grant No. 119-1193079-1084). We thank professor Guy Dodson for his kind donation of zinc-free insulin.

REFERENCES

1. S. L. Howell, W. Montague, and M. Tyhurst, *J. Cell Sci.* **19** (1975) 395–409.
2. J. Brange, (1994) *Studies on insulin stability, Stability of Insulin*, Kluwer, Academic Publishers, Dordrecht, The Netherlands, pp.17–37.
3. G. G. Dodson and D. Steiner, *Curr. Opin. Struct. Biol.* **8** (1998) 189–194.
4. N. C. Kaarsholm, H. C. Ko, and M. F. Dunn, *Biochemistry* **28** (1989) 4427–4435.
5. M. J. Adams, T. L. Blundell, E. J. Dodson, G. G. Dodson, M. Vijayan, F. H. Allen, J. E. Davies, J. J. Galloy, O. Johnson, O. Dennard, E. N. Baker, M. M. Harding, D. C. Hodgkin, R. Rimmer, and S. Sheet, *Nature* **224** (1969) 491–495.

6. D. G. Smith, W. A. Pangborn, and R. H. Blessing, *Acta Crystallogr., Sect. D* **59** (2003) 474–482.
7. D. G. Smith, W. A. Pangborn, and R. H. Blessing, *Acta Crystallogr., Sect. D* **61** (2005) 1476–1482.
8. G. Bentley, E. Dodson, G. Dodson, D. Hodkin, and D. Mercola, *Nature* **261** (1976) 166–168.
9. E. Ciszak and G. D. Smith, *Biochemistry* **33** (1994) 1512–1517.
10. J. L. Whittingham, S. Chaudhuri, E. J. Dodson, P. C. E. Moody, and G. G. Dodson, *Biochemistry* **34** (1995) 15553–15563.
11. G. D. Smith, E. Ciszak, and W. Pangborn, *Protein Sci.* **5** (1996), 1502–1511.
12. G. D. Smith, E. Ciszak, L. A. Magrum, W. A. Pangborn and R. H. Blessing, *Acta Crystallogr., Sect. D* **56** (2000) 1541–1548.
13. M. Norman and G. Schluckebier, *BMC Structural Biology* (2007).
14. C. P. Hill, Z. Dauter, E. J. Dodson, G. G. Dodson, and M. F. Dunn, *Biochemistry* **30** (1991) 917–924.
15. R. Sreekanth, V. Pattabhi, and S. S. Rajan, *Int. J. Biol. Macromol.* **44** (2009) 29–36.
16. N. R. S. Krishna, V. Pattabhi, and S. S. Rajan, *Protein Pept. Lett.* **18** (2011) 457–466.
17. B. Prugovečki, E. J. Dodson, G. G. Dodson, and D. Matković-Čaligović, *Croatica Chemica Acta* **82** (2009) 433–438.
18. B. Prugovečki, PhD Thesis, University of Zagreb, 2005.
19. J. Nicholson, L. Perkins, and F. Körber, *Recent Res. Dev. Mol. Biol.* **3** (2006) 1–16.
20. L. Di Costanzo, G. Sabio, A. Mora, P. C. Rodriguez, A. C. Ochoa, F. Centeno, D. W. Christianson, *Proc. Natl. Acad. Sci. U.S.A.* **102** (37) (2005) 13058–13063.
21. S. Jitrapakdee, M. St Maurice, I. Rayment, W. W. Cleland, J. C. Wallace, and P. V. Attwood, *Biochem. J.* **413** (2008) 369–387.
22. G. E. Borgstahl, H. E. Parge, M. J. Hickey, M. J. Johnson, M. Boissinot, R. A. Hallewell, J. R. Lepock, D. E. Cabelli, J. A. Tainer, *Biochemistry* **35** (1996). 4287–4297.
23. A. G. W. Leslie, P. Brick, and A. J. Wonacott, *CCP4 Newslett.* **18** (1986) 33–39.
24. CCP4 Collaborative Computational Project, Number 4. "The CCP4 Suite: Programs for Protein Crystallography" *Acta Crystallogr., Sect. D* **50** (1994) 760–763.
25. G. N. Murshudov, A. A. Vagin, and E. J. Dodson, *Acta Crystallogr., Sect. D* **53** (1997) 240–255.
26. V. S. Lamzir, A. Perrakis, and K. S. Wilson, *International Tables for Crystallography, Crystallography of Biological Macromolecules*, Kluwer Academic Publisher, Dordrecht, 1999, pp.720–722.
27. G. G. Langer, S. X. Cohen, A. Perrakis, and V. S. Lamzin, *Nature Protocols* **3** (2008) 1171–1179.
28. R. A. Laskowski, M. W. MacArthur, D. S. Moss and J. M. Thornton, *J. Appl. Crystallogr.* **26** (1993) 283–291.
29. W. L. DeLano, *The PyMOL Molecular Graphics System* (2002) http://www.pymol.org
30. Accelrys Software Inc., *Discovery Studio Modeling Environment, Release 3.1*, San Diego: Accelrys Software Inc., 2012
31. W. Kabsch, *Acta Crystallogr., Sect A* **32** (1976) 922–923.
32. H. M. Berman, J. Westbrook, Z. Feng, G. Gilliland, T. N. Bhat, H. Weissig, I. N. Shindyalov and P. E. Burne, *Nucleic Acid Res.* 28 (2000) 235–242. The protein DataBank, http://www.rcsb.org
33. K. Hsin, Y. Sheng, M. M. Harding, P. Taylor, and M. D. Walkinshaw, *J. Appl. Crystallogr.* **41** (2008) 963–968.
34. F. H. Allen, *Acta Crystallogr., Sect. B* 58 (2002) 380–388.